Miner Deposita (2008) 43:61–78
DOI 10.1007/s00126-007-0147-1

ARTICLE

Time relationships between volcanism–plutonism–alteration–mineralization in Cu-stratabound ore deposits from the Michilla mining district, northern Chile: a $^{40}Ar/^{39}Ar$ geochronological approach

Verónica Oliveros · Dania Tristá-Aguilera · Gilbert Féraud · Diego Morata · Luis Aguirre · Shoji Kojima · Fernando Ferraris

Received: 29 March 2006 / Accepted: 31 May 2007 / Published online: 28 July 2007

Abstract The Michilla mining district comprises one of the most important stratabound and breccia-style copper deposits of the Coastal Cordillera of northern Chile, hosted by the Middle Jurassic volcanic rocks of the La Negra Formation. $^{40}Ar/^{39}Ar$ analyses carried out on igneous and alteration minerals from volcanic and plutonic rocks in the district allow a chronological sequence of several magmatic and alteration events of the district to be established. The first event was the extrusion of a thick lava series of the La Negra Formation, dated at 159.9±1.0 Ma (2σ) from the upper part of the series. A contemporaneous intrusion is dated at 159.6±1.1 Ma, and later intrusive events are dated at 145.5±2.8 and 137.4±1.1 Ma, respectively. Analyzed alteration minerals such as adularia, sericite, and actinolite apparently give valid $^{40}Ar/^{39}Ar$ plateau and miniplateau ages. They indicate the occurrence of several alteration events at ca. 160–163, 154–157, 143–148, and 135–137 Ma. The first alteration event, being partly contemporaneous with volcanic and plutonic rocks, was probably produced in a high thermal gradient environment. The later events may be related either to a regional low-grade hydrothermal alteration/metamorphism process or to plutonic intrusions. The Cu mineralization of the Michilla district is robustly bracketed between 163.6±1.9 and 137.4±1.1 Ma, corresponding to dating of actinolite coexisting with early-stage chalcocite and a postmineralization barren dyke, respectively. More precisely, the association of small intrusives (a dated stock from the Michilla district) with Cu mineralization in the region strongly suggests that the main Michilla ore deposit is related to a magmatic/hydrothermal event that occurred between 157.4±3.6 and 163.5±1.9 Ma, contemporaneous or shortly after the extrusion of the volcanic sequence. This age is in agreement with the Re–Os age of 159±16 Ma obtained from the mineralization itself (Tristá-Aguilera et al., *Miner Depos*, 41:99–105,2006).

Keywords Geochronology · Cu-stratabound deposits · Northern Chile · Jurassic · Coastal Cordillera

Editorial handling: R. King

V. Oliveros (✉) · D. Morata · L. Aguirre
Departamento de Geología, Universidad de Chile,
P.O. Box 13518-21, Santiago, Chile
e-mail: volivero@ing.uchile.cl

D. Tristá-Aguilera · S. Kojima
Departamento de Ciencias Geológicas,
Universidad Católica del Norte,
Av Angamos 0610, Casilla 1280,
Antofagasta, Chile

G. Féraud
CNRS-IRD-UNSA UMR 6526 Géosciences Azur, Parc Valrose,
Université de Nice-Sophia Antipolis,
06108 Nice, France

F. Ferraris
Superintendencia de Geología, Minera Michilla S.A.,
km 110 camino a Tocopilla,
Mejillones, Segunda Región de Antofagasta, Chile
e-mail: fferraris@vtr.net

Present address:
V. Oliveros
Departamento de Ciencias de la Tierra,
Universidad de Concepción,
P.O. Box 160-C, Concepción, Chile

Introduction

Cu-stratabound ore deposits along the Coastal Cordillera in northern Chile form the third source of copper production in Chile (Maksaev and Zentilli 2002) and are mostly hosted by thick Jurassic (La Negra Formation) and Lower Cretaceous volcano-sedimentary formations. The volcano-sedimentary formations were episodically intruded by calc-alkaline granitoids (from diorite to granodiorite) and dykes during the Late Jurassic and Early Cretaceous (Rogers 1985; Chavez 1985; Pichowiak 1994; Dallmeyer et al. 1996; Oliveros et al. 2006). Volcanic and, to a minor extent, plutonic rocks were affected by regional very low-grade hydrothermal alteration or metamorphic processes and/or by local hydrothermal alteration processes most often associated with mineralization (Losert 1974; Oliveros 2005). Available K–Ar and Rb–Sr radiometric data indicate ages around 150–140 Ma for the main stratabound deposits hosted by Jurassic volcano-sedimentary rocks in northern Chile (see Maksaev and Zentilli 2002 and references therein), younger than those assumed for volcanism (see below) but overlapping ages of plutonism. The previous isotopic ages have been obtained from whole rocks and, in a few cases, from minerals such as plagioclase, biotite, and amphibole separated from intrusive and volcanic rocks. Nevertheless, the time interval is imprecise and must be considered with caution because: (1) The analyzed material is most often whole rock, which is always altered in the Coastal Cordillera, and the K–Ar and Rb–Sr systems are very sensitive to alteration, and (2) the associated errors are higher than 2% and can reach 10%. Taking into account the uncertainties in the reported age data, the time interval for the formation of the stratabound Cu deposit is more likley 172–138 Ma. Available Rb–Sr and K–Ar whole-rock radiometric data performed on diorites and andesitic lava flows of the Michilla district constrain the mineralization between ca. 192 and 146 Ma (Astudillo 1983; Venegas et al. 1991).

Several syngenetic vs epigenetic models for the genesis of these Cu-stratabound deposits have been proposed (see Maksaev and Zentilli 2002). Nevertheless, an epigenetic model is currently preferred based on the relationships observed between plutonism and hydrothermal alteration.

In this study, we present new $^{40}Ar/^{39}Ar$ radiometric ages on volcanism, plutonism, regional alteration, and local alteration for the Cu-stratabound ore deposits from the Michilla district in northern Chile. This district is one of the largest in the Cu-stratabound metallogenetic province and includes lava flows of the La Negra Formation, subvolcanic intrusions, plutonic bodies from the Coastal Batholith, and some of the largest Cu-stratabound deposits of the province (Fig. 1). Lince–Estefanía is the most important ore body in the Michilla District, and its geology has been recently studied in detail (Acevedo 2002; Tristá-Aguilera et al. 2006; Tristá-Aguilera 2007). A recent Re–Os age of 159±16 Ma (2σ) obtained from the main Cu-sulfides mineralization at the Lince–Estefanía deposit represents the first direct age obtained from the primary sulfides of the Cu-stratabound ore deposits (Tristá-Aguilera et al. 2006).

The aim of this study is to constrain the ages of the successive geological processes that affected a district where typical Cu-stratabound deposits developed. Consequently, this study contributes to a better understanding of Jurassic–Early Cretaceous evolution of the present Coastal Cordillera, northern Chile. By dating various igneous and alteration events of the district, we bracket the age of Cu mineralization more precisely than previously done. These data represent crucial information that are necessary for models explaining Cu-stratabound deposit formation.

Geological and Tectonic setting

During Jurassic to Early Cretaceous times, subduction-related magmatism developed along the present Coastal Cordillera of northern Chile. The main products of this magmatic activity are thick volcanic sequences and plutonic rocks emplaced under low-pressure conditions (Dallmeyer et al. 1996). The volcanic sequence, defined as the La Negra Formation (García 1967), was emplaced on a thinned pre-Jurassic continental crust as a consequence of an extreme oblique movement of the Phoenix Plate in a south–southeastern direction relative to the South American continental margin (e.g., Scheuber and González 1999). This formation consists mainly of andesitic–basaltic lavas and variable amounts of tuff breccias, sandstone, and limestone (García 1967). Rogers and Hawkesworth 1989 reported a Rb–Sr isochron age of 186.3±13.6 Ma (1σ). Recently, Oliveros et al. 2006, 2007) have reported $^{40}Ar/^{39}Ar$ plateau ages of ca. 150–152 (23°49′S, Antofagasta city area), 160–164 (22°29′S, south of Tocopilla), and 156 Ma (23°39′, Mantos Blancos mining area) on mineral separates (Fig. 1).

Along the entire Coastal Range in northern Chile, the La Negra Formation is extensively intruded by numerous plutonic bodies of gabbroic to granitic composition, grouped in the so-called Coastal Batholith. The ages obtained from these bodies range from ca. 142 to 168 Ma (Rogers 1985; Espinoza and Orquera 1988; Boric et al. 1990; Maksaev 1990; Oliveros 2005; Oliveros et al. 2006). In addition, dioritic to gabbroic dikes and stocks intrude the volcanic sequence. These smaller intrusions were dated by the K–Ar and Rb–Sr methods (whole-rock and plagioclase) between 112 and 168 Ma (e.g., Astudillo 1983; Espinoza and Orquera 1988; Boric et al. 1990; Venegas et al. 1991; Maksaev 1990). Semiconsolidated coarse-grained sediments of Cenozoic age (e.g., Boric et al. 1990) overlie these igneous rocks.

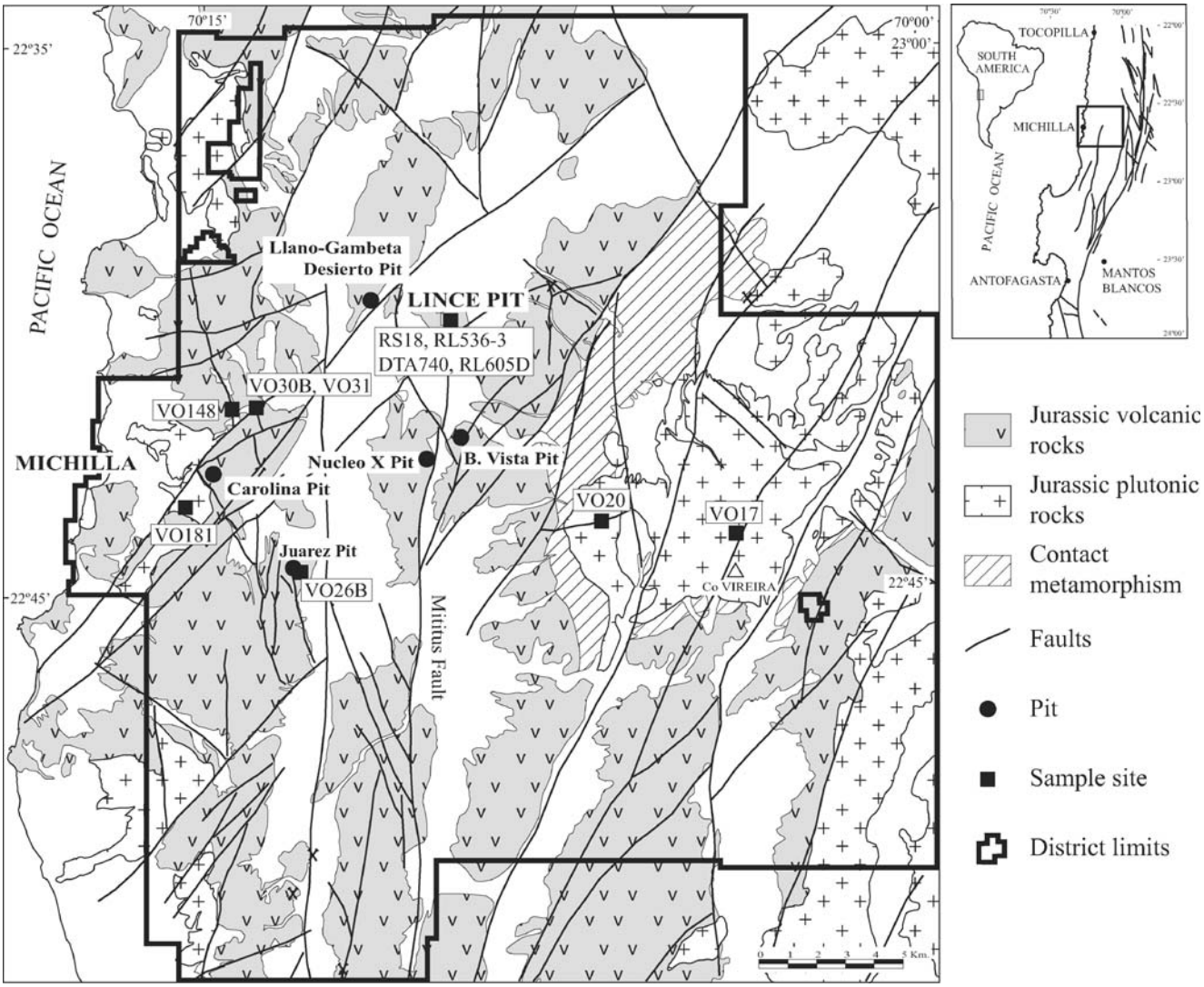

Fig. 1 Simplified geology of the Michilla minig district and location of sampled rocks. Modified from the geological map of Michilla Mining

Both plutonic and volcanic units were affected by regional scale low- to very low-grade alteration events. The main products of these alteration events are chorite, epidote, quartz, sericite, titanite, calcite, and minor amounts of zeolites, prehnite, pumpellyite, and actinolite. A combination of processes such as burial metamorphism or heating and fluid contribution from the intrusion of the Coastal Batholith have been advocated for the origin of these alteration events (Losert 1974; Sato 1984; Oliveros 2005). Preliminary ages obtained from secondary minerals associated with these events range between ca. 160 and 100 Ma (Oliveros 2005).

The most important structural feature is the major 1,000-km-long (21–30°S) Atacama Fault System (AFS), mainly consisting of north-to-south-oriented trench-linked faults. The AFS is thought to have formed during the Late Jurassic and Early Cretaceous as an intra-arc regional structure related to oblique subduction of the Aluk (Phoenix) plate relative to the South American continent (e.g., Scheuber and González 1999). The geometry, kinematics, and timing of deformation of the AFS are well known at a regional scale (see Cembrano et al. 2005 and references therein). Changes from intra-arc sinistral transtensional to sinistral transpressional deformation are thought to have occurred during arc construction and AFS evolution at least from 190 to 110 Ma (Cembrano et al. 2005). Apatite fission track ages between 129 and 92 Ma (Maksaev 2000) on Jurassic granitoids from the Coastal Range in northern Chile indicate a low exhumation rate for this segment of the Cordillera from the Early Cretaceous and limits the maximum stratigraphic pile responsible for the regional low-grade metamorphism that probably affected the volcanic rocks of the La Negra Formation.

Geology of the Michilla district

The Michilla district represents one of the largest and most important districts in the Cu-stratabound metallogenetic

province between 22 and 26° Latitude south. The outcropping units in the district correspond to basaltic to andesitic lava flows with amygdaloidal, porphyritic, afanitic, or brecciated textures, intercalated with lesser amounts of tuff breccias, sandstones and limestones (Niemeyer et al. 1990, Bogdanic et al. 1994), subvolcanic and plutonic bodies, and sedimentary covers. The lava flows form a structure varying in orientation from northeast, in the west, to northwest in the central and eastern area of the district, with an overall northerly dip. Plutonic rocks are represented by gabbro-diorites to monzonites and granodiorites, forming north-to-south-oriented belts with some isolated intrusions (e.g., Cerro Vireira, Fig. 1). In addition, subvolcanic intrusions of gabbroic–dioritic composition were emplaced along a dominantly northeastern orientation (Fig. 2). The geological units are mostly affected by branches of the AFS, the most important of which has a north-to-south orientation (e.g., the Mititus Fault System), but minor northeastern and northwestern faults are also observed.

The copper ore bodies generally surround intrusive bodies and form stratiform (e.g., Lince–Estefanía, Buena Vista, Desierto, and Juárez deposits; Fig. 1) and breccia bodies (e.g., Lince–Estefanía and Llano–Gambeta deposits; Fig. 2). In addition, ore minerals are sometimes exposed as irregular, structurally controlled bodies (e.g., Carolina, Núcleo X deposits). The ore bodies were formed during three stages: hypogene (early, main and late substage), supergene, and oxide (Kojima et al. 2003). The ore minerals consist mainly of Cu sulfides and oxides. Copper sulfides are represented by chalcocite (hypogene and supergene), bornite, covellite, and chalcopyrite, whereas Cu oxides are dominanted by atacamite and chrysocolla (Fig. 3a). The ore minerals display a vertical zoning with sulfide phases occurring in the deepest levels (below 250 m above sea level [m.a.s.l.]) and oxides dominating near the surface (above 500 m.a.s.l.). A mixed-ore zone (oxide–sulfide) occurs between these two levels. Cu oxides also occur in trace amounts throughout the whole mineralized column (~1,000 m currently recognized). The alteration minerals related to the main Cu sulfide mineralization are chlorite, epidote, and albite, with scarce quartz and actinolite (Wolf et al. 1990; Kojima et al. 2003; Tristá-Aguilera 2007; Fig. 3a), whereas the alteration mineral assemblage related to the Cu oxide mineralization is calcite and gypsum with minor quartz.

Lince–Estefanía is the most important ore body of the Michilla district. It is located in N60°E/45°NW-oriented lava flows consisting of brecciated, aphanitic, porphyritic, and amygdaloidal andesites. Widespread northeast-oriented dykes and small gabbroic to dioritic stocks are also present (Fig. 2). Field and petrographic observations indicate the

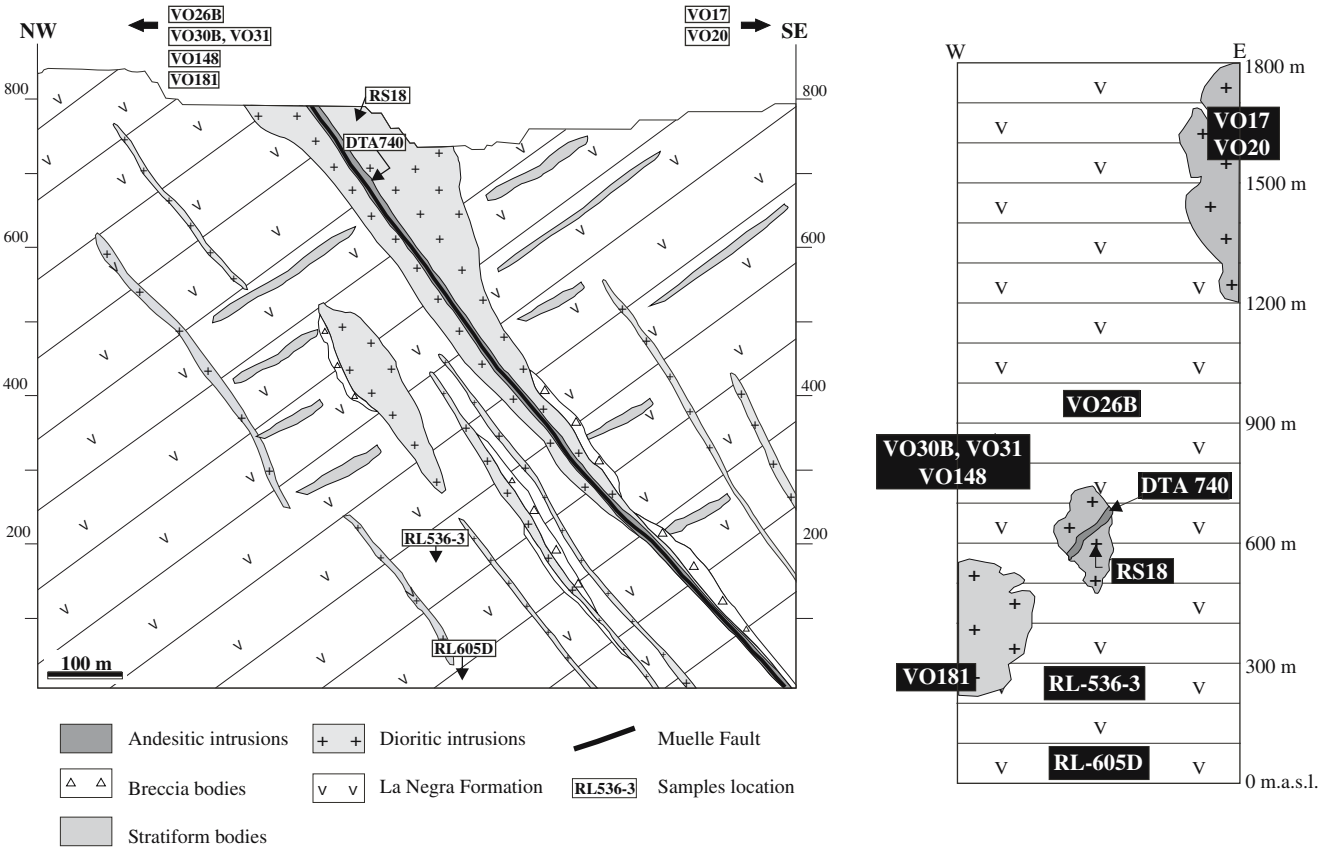

Fig. 2 Schematic cross-section of the Michilla mine and synthetic column of the Michilla district (Coastal Range, northern Chile) with location of samples. On the synthetic column, the samples are located relative to their altitude and not to their stratigraphic position

a

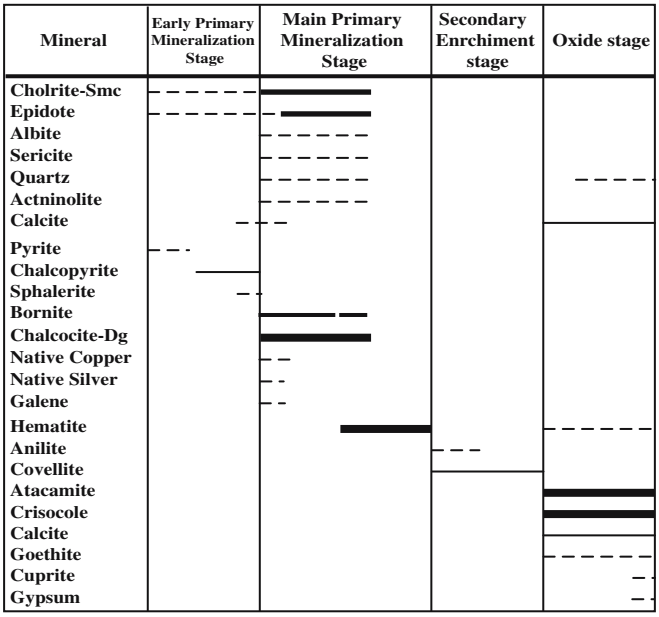

b

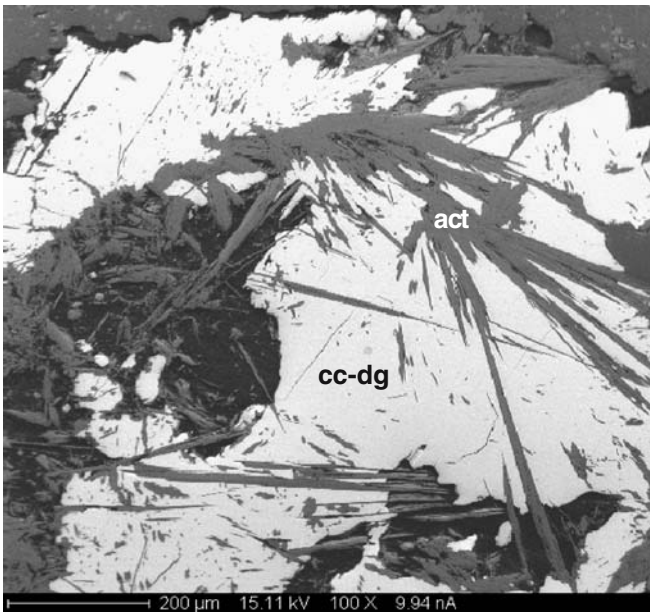

Fig. 3 **a** Paragenetic sequence of ore and gangue minerals observed in the Lince–Estefanía deposit, modified after Kojima et al. (2003) and Tristá-Aguilera 2007. **b** Backscattered electron image of an amygdale from a lava flow inside the Lince pit. *act* Actinolite, *cc* chalcocite, *dg* digenite, *smc* smectite

occurrence of at least two types of intrusions: (a) premain hypogene mineralization two-pyroxene calc-alkaline diorites and (b) postmain hypogene mineralization porphyritic hornblende-bearing calc-alkaline andesitic dykes. In this deposit, ore minerals form stratiform and breccia bodies. The stratiform bodies are close but peripheral to intrusions (dioritic stocks), whereas breccia bodies surround dioritic stocks and grade into stratiform bodies. The main breccia body extending from the surface to about 900 m depth is formed by volcanic and intrusive fragments with ore and alteration minerals forming the matrix. The occurrence of intrusive fragments within breccias indicates that some intrusions predate the main hypogene mineralization event, but the geometrical relationships between breccia and intrusions (as shown in Fig. 2) suggest that both are genetically related.

Description of the analyzed samples

Volcanic host rocks (La Negra Formation)

Sample VO26B is an andesite lava flow sampled from inside the Juarez pit (Fig. 1) with numerous amygdales and veins filled with alteration mineral phases, but no traces of ore minerals are observed. VO30B, VO31, and VO148 samples belong to a 500-m-thick sequence of lava flows and minor intercalated sedimentary rocks at a distance of about 5 km from any copper deposit (Fig. 1), whereas RL536-3 and RL605D samples of lava flows were obtained from drill cores of the main deposit in the district (Fig. 2).

The stratigraphic position of VO26B, relatively to VO30B, VO31, and VO148, is unknown, whereas sample VO148 is stratigraphically located 50 m above VO30B and VO31. These three samples are stratigraphically located about 500 and 700 m above samples RL536-3 and RL605D, respectively (Figs. 1 and 2).

Phenocrysts in the sampled volcanic rocks are mainly plagioclase ($An_{64.8–48.2}Ab_{48.9–38.3}Or_{3.3–1.4}$), clinopyroxene, and iron oxide (magnetite). The groundmass is composed of plagioclase microlites, mafic minerals, iron oxides, and recrystallized glass. Secondary mineral phases are ubiquitous in the volcanic rocks and some plutonic rocks. Plagioclase phenocrysts are often albitized, replaced by sericite, minor mafic philosilicates and, as in the case of sample VO148, prehnite and calcite. Mafic phenocrysts are partially or completely replaced by chlorite. Glass in the groundmass is recrystallized to chlorite and other mafic silicates, titanite and quartz. Amygdales and veins filled with chlorite, epidote, quartz, and potassic feldspar are present. Calcite seems to be a later alteration phase because it was formed in the center of the amygdales or in veins covering or cutting other alteration minerals. Amygdales and veins filled with epidote, actinolite, and chlorite are observed in sample RL536-3.

Intrusive rocks

RS18 is a prehypogene mineralization microdiorite sampled from inside the Lince pit (Figs. 1 and 2). It is mostly barren and composed of orthopyroxene ($En_{71.7–73.9}Fs_{22.7–24.1}$

$Wo_{3.4–4.0}$), clinopyroxene ($En_{38.5–45.2}Fs_{18.0–22.5}Wo_{34.7–41.1}$), plagioclase ($An_{46.1–61.1}Ab_{37.5–51.7}Or_{0.9–2.6}$), and scarce, minute biotite. It has a phaneritic equigranular texture, and the grain size is 1–5 mm. Alteration consists of minor sericitization of plagioclase and partial replacement of biotite by mafic phyllosilicates. DTA-740 is an andesitic dyke sampled from the pit and composed of zoned idiomorphic hornblende amphibole and plagioclase (completely altered to fine-grained clay minerals) phenocrysts in an altered groundmass. This dyke is barren and crosscuts the Lince pit orebodies.

Other intrusions were also sampled in the eastern (samples VO17 and VO20 from Cerro Vireira, which belong to the same plutonic complex) and western (VO181) borders of the district (Figs. 1 and 2). They are granodiorite (VO17, VO20) and diorite (VO181) composed of plagioclase, K-feldspar, quartz, pyroxene—which could be replaced by either hornblende during cooling processes or fibrous actinolite corresponding to later alteration processes—and magnetite. They have a phaneritic equigranular texture with a grain size of 5–10 mm. Plagioclases are weakly sericitized and albitized and could contain small grains of epidote; K-feldspars are altered to clay minerals. Titanite and epidote are present as secondary minerals partially replacing the pyroxene and magnetite crystals. In sample VO181, tourmaline is also present as a late mineral.

Analytical procedures

Thirteen primary and secondary minerals were analyzed by the step-heating Ar–Ar method from 11 rock samples. They were small bulk sample plagioclase (VO31, VO148: around 200 grains, and VO17, VO20, RS18: around 30 grains), potassic feldspar (adularia), single grains collected from amygdales (VO26B, VO30B), and strongly sericitized plagioclase single grains (VO31, VO148, RS18, RL605D), all heated with a CO_2 Synrad 48–50 laser. Bulk sample primary amphibole (DTA740) and secondary actinolite (RL536D-3) were heated with a high frequency (HF) furnace. Mineral separation was carried out using a Frantz magnetic separator and finally by careful hand picking under a binocular microscope. Grain sizes were 200–500 (sericitized plagioclase and adularia single grains), 125–200 (amphibole and fresh plagioclase bulk samples), and below 50 μm (diameter) for the fibrous actinolite bulk sample. The weight of the analyzed samples was 0.01–0.05 mg for adularia and sericitized plagioclase single grains, ~0.1–1.2 mg for the plagioclase bulk sample heated with the laser system, 10.9 mg for the amphibole, and 20.7 mg for the actinolite bulk samples analyzed with the HF furnace. The samples were packed into copper (for HF furnace experiments) or aluminum foils (for laser experiments) and irradiated for 70.0 h in the Hamilton McMaster University nuclear reactor (Canada) in position 5C along with Hb3gr hornblende neutron fluence monitor for which an age of 1,072 Ma is adopted (Turner et al. 1971; Renne et al. 1998, Jourdan et al. 2006). The total neutron flux density during irradiation was around 8.8×10^{18} neutrons/cm^2. The estimated error bar on the corresponding $^{40}Ar^*/^{39}Ar_K$ ratio was ±0.4% (2σ) in the volume where the samples were included. For laser-heating experiments, isotopic measurements were performed with a VG3600 mass spectrometer working with a Daly system and a photomultiplier. For HF-heating experiments, isotopic analyses were performed with a double-vacuum HF furnace and a mass spectrometer composed of a 120° M.A.S.S.E. tube, a Baür–Signer GS 98 source, and a SEV217 Balzers electron multiplier. Total blanks were measured at every third step on the laser system and on every third sample on the HF furnace system. Argon isotopes were typically on the order of 10–2,450, 30–15,700, and 1–70 (laser experiments), and 30–430, 10–7,000, and 8–50 (HF furnace experiments) times the blank level for ^{40}Ar, ^{39}Ar, and ^{36}Ar, respectively.

The criteria to define a plateau age are: (1) at least 70% of the ^{39}Ar released, (2) a minimum of three successive steps in the plateau, and (3) the integrated age of the plateau should agree with each apparent age of the plateau within a two sigma (2σ) confidence level. Miniplateau age concerns a fraction lower than 70% of ^{39}Ar released. The uncertainties on the $^{40}Ar/^{39}Ar$ ratios of the monitors are included in the calculation of the integrated and plateau age uncertainties, but the error on the age of the monitor is not included. Error bars on plateau ages are given at the 2-sigma level. Chemical compositions of primary and secondary minerals were obtained using a CAMECA SX-100 electron microprobe with 20 kV, 10 nA, and 2–5 μm as analytical conditions, at the Institut des Sciences de la Terre, de l'Environnement et de l'Espace of the University of Montpellier (France).

Results

Summarized and detailed isotopic data are given in Tables 1 and 2, respectively. Age and $^{37}Ar_{Ca}/^{39}Ar_K$ ratio spectra are shown in Figs. 4 and 5. Electron microprobe Ca/K ratios for fresh plagioclase ($An_{67–49}Ab_{49–31}Or_{3–1}$) are listed in Table 3. Isochron data are given in Table 2, but they are not plotted because the data are too clustered to provide useful information.

Magmatic minerals

Plagioclase

The plagioclase sample VO31 yields a disturbed age spectrum consisting of a flat low-temperature part with a weighted mean

age (w.m.a.) of 153.7±1.8 Ma, 50% of the ^{39}Ar released, followed by increasing ages vs temperature (Fig. 4a). The oldest ages correlate with the highest $^{37}Ar_{Ca}/^{39}Ar_K$ ratios representing the freshest plagioclase, as shown by Ca/K values measured with the microprobe. It is therefore likely that (1) the high temperature w.m.a. of 163.6±1.8 Ma represents the best estimate of the age of this lava flow and (2) the low-temperature ages are the result of a sericite/plagioclase mixture.

Plagioclase sample VO148 yields a plateau age of 159.9±1.0 Ma (Fig. 4b, 85.6% of the gas released), slightly younger than the high-temperature age of VO31. The corresponding $^{37}Ar_{Ca}/^{39}Ar_K$ ratios increase with temperature but remain in the range given by microprobe analyses for fresh plagioclase.

The bulk sample plagioclases VO17 and VO20 yield concordant plateau ages of 147.1±2.2 and 145.5±2.8 Ma (Figs. 4c,d), respectively. Whereas the corresponding $^{37}Ar_{Ca}/^{39}Ar_K$ ratios for the sample VO20 plateau fraction correspond to fresh plagioclase, the VO17 plateau age may correspond to a mixture of fresh plagioclase and sericite. Moreover, the isochron data are more precise for the VO20 sample (Table 2). Therefore, the plateau age obtained for sample VO20 is preferred for the cooling age of this pluton. The large variation of the Ca/K ratios (measured with the microprobe) observed in sample VO20 could be explained partly by the zoning of the plagioclase crystals, which vary in composition from An_{40} to An_{70} (Oliveros 2005).

Plagioclase sample VO181 yields a plateau age of 159.6±1.1 Ma correlating with a flat $^{37}Ar_{Ca}/^{39}Ar_K$ ratio spectrum (Fig. 4e), which demonstrates that the analyzed plagioclase was mostly pure.

Finally, plagioclase bulk sample RS18 from the main dioritic stock located inside the Lince pit (Fig. 2) displays two concordant plateau ages of 154.4±3.9 and 153.7±3.2 Ma (Fig. 4f) affected by large error bars because of the low quantity of analyzed grains. Nevertheless, we observe a slight increase in apparent ages that appear to be correlated with the $^{37}Ar_{Ca}/^{39}Ar_K$ ratios. It is therefore likely that the best estimate of the closure age of these plagioclases is given by high-temperature ages of 157.8±5.6 and 157.0±5.0 Ma (w.m.a.=157.4±3.7 Ma). This age is concordant with the VO181 plateau age. Single grains of strongly seritized plagioclase were analyzed by two-step experiments, and the data are given below.

Amphibole

Amphibole (hornblende) sample DTA-740 (Lince Pit barren dyke) yields a plateau age of 137.4±1.1 Ma, probably corresponding to pure amphibole, as shown by the flat $^{37}Ar_{Ca}/^{39}Ar_K$ ratio spectrum (Fig. 4g).

Alteration minerals

Adularia

Adularia single grains from amygdales sample VO26B yield two concordant plateau ages of 139.6±1.5 and 137.6±2.2 Ma, corresponding to flat and variable $^{37}Ar_{Ca}/^{39}Ar_K$ ratios (Fig. 5a). An adularia single grain from sample VO30B displays a plateau age of 145.1±0.7 Ma (Fig. 5b), concordant with a miniplateau age of 143.8±1.1 Ma (65% of ^{39}Ar released) obtained from another grain. The very low and mostly constant $^{37}Ar_{Ca}/^{39}Ar_K$ ratios demonstrate that the analyzed adularia grains were pure.

Sericitized plagioclase

Because of their tiny size, secondary minerals such as sericite could not be separated from the plagioclase host mineral and therefore were analyzed by heating single grains of strongly altered plagioclase where sericite represents the dominant secondary mineral. Aguirre et al. 1999 and Fuentes et al. 2005 showed that the obtained plateau ages may represent the age of the sericite in some cases, the contribution of fresh plagioclase being negligible because of the much lower K content. Sericitized plagioclase single grains from sample VO31 yield concordant plateau ages of 157.9±3.8 and 154.6±2.6 Ma (Fig. 5c). The rather high and variable $^{37}Ar_{Ca}/^{39}Ar_K$ ratios show that these grains probably contained low proportions of sericite; this explains the large error bars because of small argon signals during measurements. Nevertheless, these ages are concordant with the low-temperature w.m.a of 153.7±1.8 Ma obtained from "fresh" plagioclase. Single grains of sericitized plagioclase sample VO148 yield concordant plateau ages of 160.9±1.4 and 161.2±0.9 Ma (Fig. 5d), which are concordant with the plateau age (159.9±1.0 Ma) obtained from fresh plagioclase.

Single grains of strongly sericitized plagioclase sample RS18 (dioritic stock inside the Lince pit) were too small to perform step-heating experiments. Therefore, 11 single grains of sericitized plagioclase were individually heated in two steps only. The first step allows degassing of atmospheric argon and the second one—total fusion—generally represents ~90% of the radiogenic argon released. When plotting these ages and apparent ages from small clusters of step-heated "fresh" plagioclase (Fig. 4f) vs $^{37}Ar_{Ca}/^{39}Ar_K$ ratios (Fig. 6), a positive correlation is observed, indicating that the lower the $^{37}Ar_{Ca}/^{39}Ar_K$ ratio of the analyzed material, the younger is the obtained age. According to the correlation trend, the age of a pure sericite would be on the order of 148 Ma, corresponding to a low (near zero) $^{37}Ar_{Ca}/^{39}Ar_K$ ratio, whereas the "pure" plagioclase age would be estimated around 158 Ma (Fig. 6).

Table 1 Summary of $^{40}Ar/^{39}Ar$ data on plagioclase, amphibole, sericitized plagioclase, adularia, and actinolite from lava flows and intrusives from the Michilla mining district

Step number or T (°C)	Atmospheric (%)	^{39}Ar (%)	$^{37}Ar_{Ca}/^{39}Ar_K$	$^{40}Ar^*/^{39}Ar_K$	Age±1σ (Ma)
VO17 Plagioclase, 30 grains (J=0.01607)					
1	97.4	0.5	3.5	1.902	54.3±87.6
2	53.9	3.3	3.8	4.654	130.1±13.5
3	29.8	17.6	5.0	5.130	142.9±2.4
4	20.6	17.6	4.2	5.388	149.8±2.4
5	27.6	22.0	4.9	5.351	148.9±2.2
6	24.6	19.8	4.3	5.295	147.4±2.6
7	30.6	19.2	6.1	5.249	146.1±2.6
VO20 Plagioclase, 30 grains (J=0.01608)					
1	80.9	0.9	4.7	7.002	192.5±66.5
2	72.5	2.1	11.0	5.341	148.6±21.3
3	58.7	5.7	13.2	5.262	146.5±8.5
4	39.1	8.0	13.9	5.146	143.4±4.8
5	20.2	9.7	13.9	5.408	150.4±3.9
6	32.8	12.7	13.0	5.145	143.4±3.8
7	17.5	24.6	15.7	5.219	145.4±2.0
8	28.6	8.9	15.0	5.165	143.9±5.1
9	41.1	6.7	13.8	4.934	137.7±9.3
10	16.0	20.8	16.9	5.324	148.2±2.4
VO26B (1) K-Feldspar, single grain, 0.04 mg (J=0.01758)					
1	10.0	4.7	0.001	4.410	134.7±1.4
2	6.7	1.3	0.000	4.670	142.3±4.2
3	1.3	2.0	0.000	4.830	147.0±3.0
4	18.4	2.8	0.001	4.550	138.8±1.9
5	55.2	53.1	0.001	4.518	137.9±1.1
6	57.9	11.3	0.001	4.574	139.5±1.7
7	53.0	24.9	0.001	4.704	143.3±1.3
VO26B (2) K-Feldspar, single grain, 0.01 mg (J=0.01758)					
1	22.5	8.4	0.000	4.528	138.2±3.6
2	9.1	2.5	0.002	4.748	144.6±9.7
3	12.7	2.4	0.001	4.556	139.0±11.3
4	11.7	1.0	0.000	5.323	161.4±23.0
5	43.1	5.0	0.000	4.735	144.2±5.3
6	58.7	37.4	0.000	4.468	136.4±1.9
7	58.6	27.7	0.001	4.470	136.5±1.6
8	59.5	8.5	0.003	4.561	139.1±3.0
9	56.8	7.1	0.002	4.646	141.6±4.0
VO30B (1) K-Feldspar, single grain, 0.02 mg (J=0.01758)					
1	78.2	1.6	11.0	3.667	112.5±9.8
2	33.4	3.5	16.9	4.490	136.8±3.8
3	14.6	14.6	16.5	4.597	139.9±1.4
4	10.2	12.6	16.9	4.538	138.2±1.1
5	7.8	7.8	17.6	4.670	142.0±2.0
6	9.4	5.7	17.9	4.602	140.0±2.3
7	14.6	8.4	18.2	4.514	137.5±2.2
8	18.7	11.8	17.3	4.469	136.2±1.4
9	17.5	11.9	18.8	4.699	142.9±1.3
10	11.3	12.1	21.5	5.008	151.9±1.2
11	12.6	10.1	22.0	4.971	150.8±1.4
VO30B (2) K-Feldspar, single grain, 0.01 mg (J=0.01758)					
1	16.1	4.0	0.0	4.829	147.0±2.0
2	23.4	5.2	0.0	4.776	145.5±1.7
3	27.2	33.5	0.0	4.732	144.2±0.6
4	27.1	30.1	0.0	4.764	145.1±0.6
5	28.0	11.7	0.0	4.782	145.6±0.8
6	28.0	8.1	0.0	4.790	145.9±1.2

Table 1 (continued)

Step number or T (°C)	Atmospheric (%)	^{39}Ar (%)	$^{37}Ar_{Ca}/^{39}Ar_K$	$^{40}Ar^*/^{39}Ar_K$	Age±1σ (Ma)
7	29.2	4.9	0.0	4.788	145.8±2.0
8	28.9	1.7	0.0	4.851	147.6±4.2
9	25.3	0.9	0.0	4.996	151.9±7.2
VO31 Plagiolcase, small bulk sample, 1.20 mg (J=0.01756)					
1	67.2	1.1	2.0	4.748	144.4±12.0
2	55.1	1.9	4.3	4.568	139.2±7.5
3	18.4	8.2	6.3	5.128	155.5±1.6
4	8.4	14.5	8.3	5.089	154.4±1.6
5	8.2	11.2	9.5	5.078	154.1±1.8
6	8.4	12.7	10.0	5.096	154.6±1.7
7	7.5	11.1	10.1	5.267	159.6±1.5
8	6.6	9.0	10.9	5.337	161.6±1.4
9	7.4	11.0	11.1	5.397	163.3±1.8
10	8.1	6.8	11.4	5.361	162.3±2.8
11	7.1	12.5	11.9	5.494	166.1±1.3
VO31 (1) Sericite in situ in plagioclase, single grain, 0.04 mg (J=0.01752)					
1	50.0	1.7	0.6	4.553	138.5±28.8
2	49.0	8.2	1.0	5.186	157.0±8.3
3	2.9	14.7	1.6	5.561	167.8±4.0
4	6.2	34.1	1.2	5.143	155.7±2.3
5	2.7	10.3	2.6	5.278	159.6±9.1
6	5.1	11.7	3.7	5.261	159.1±5.4
7	7.4	9.9	2.4	5.093	154.3±4.6
8	9.6	9.3	6.6	5.108	154.7±6.7
VO31 (2) Sericite in situ in plagioclase, single grain, 0.01 mg (J=0.01752)					
1	48.2	9.4	0.4	4.929	149.5±7.0
2	8.0	8.6	0.8	5.202	157.4±6.3
3	8.4	26.2	1.0	5.158	156.2±2.0
4	5.8	16.5	1.2	5.137	155.5±2.7
5	8.9	29.8	1.6	5.062	153.4±1.3
6	25.8	2.4	2.4	4.098	125.2±19.0
7	13.4	7.0	4.1	4.926	149.4±8.3
VO148 Plagiolcase, small bulk sample, 1.10 mg (J=0.01670)					
1	91.2	0.4	2.9	1.696	50.4±30.5
2	53.1	1.8	7.1	5.593	161.1±6.8
3	27.6	4.3	9.9	5.344	154.2±4.1
4	11.1	7.9	11.5	5.670	163.2±2.1
5	7.9	9.1	12.4	5.569	160.4±1.7
6	4.7	6.3	13.5	5.604	161.4±2.3
7	9.3	6.8	13.3	5.425	156.5±1.4
8	10.0	8.3	13.4	5.426	156.5±1.4
9	7.9	8.9	14.2	5.514	158.9±1.5
10	7.8	10.6	14.2	5.573	160.5±1.8
11	8.1	7.6	14.6	5.495	158.4±1.8
12	5.5	4.0	15.2	5.550	159.9±3.4
13	6.2	5.4	15.3	5.551	160.0±1.8
14	5.2	6.6	15.3	5.651	162.7±1.7
15	5.0	12.0	15.5	5.632	162.2±0.9
VO148 (1) Sericite in situ in plagioclase, single grain, 0.02 mg (J=0.01682)					
1	76.2	1.6	0.3	3.737	110.0±14.2
2	21.9	3.1	0.4	5.495	159.5±6.9
3	10.0	21.9	0.2	5.608	162.6±1.1
4	3.6	7.9	0.2	5.651	163.8±2.9
5	1.1	5.7	0.2	5.723	165.8±3.5
6	3.3	13.0	0.2	5.592	162.2±1.7
7	5.0	13.4	0.2	5.507	159.8±1.9
8	6.7	4.0	0.3	5.475	158.9±6.0

Table 1 (continued)

Step number or T (°C)	Atmospheric (%)	^{39}Ar (%)	$^{37}Ar_{Ca}/^{39}Ar_K$	$^{40}Ar^*/^{39}Ar_K$	Age±1σ (Ma)
9	9.5	6.3	0.3	5.386	156.4±3.7
10	6.5	23.1	0.3	5.457	158.4±1.0
VO148 (2) Sericite in situ in plagioclase, single grain, 0.02 mg (J=0.01682)					
1	80.5	0.7	0.1	3.314	97.9±28.8
2	36.2	2.1	0.2	4.932	143.8±8.3
3	15.0	20.0	0.1	5.579	161.8±1.2
4	3.9	34.3	0.0	5.581	161.9±0.7
5	4.2	15.5	0.1	5.526	160.3±1.1
6	3.9	7.1	0.1	5.555	161.1±2.0
7	11.3	2.7	0.3	5.452	158.3±2.9
8	6.0	17.7	0.1	5.523	160.3±0.7
RS18 Plagioclase 30 grains (J=0.01599)					
1	41.1	10.6	9.1	5.472	151.3±9.5
2	20.8	9.8	10.7	5.398	149.4±6.6
3	16.2	17.4	10.9	5.565	153.8±4.2
4	22.4	27.0	13.4	5.544	153.3±3.4
5	19.8	35.2	16.6	5.716	157.8±2.8
RS18 Plagioclase 30 grains (J=0.01599)					
1	82.1	2.6	11.6	4.195	117.1±21.6
2	41.5	13.3	13.6	5.195	144.0±6.3
3	30.6	27.7	13.3	5.443	150.6±2.1
4	25.8	21.1	13.0	5.730	158.2±3.5
5	21.3	35.4	15.0	5.686	157.0±2.5
RS18 Sericite in situ in plagioclase, 11 grains (J=0.01601)					
1	69.8	1.7	2.9	4.392	122.6±15.6
	10.8	43.8	1.5	5.312	147.2±0.8
2	57.9	0.3	4.0	3.806	106.7±50.5
	49.5	1.8	9.7	5.407	149.8±7.4
3	76.6	1.2	4.7	5.085	141.2±12.9
	27.7	20.0	3.9	4.387	122.5±1.1
4	77.0	0.4	11.2	4.664	129.9±42.7
	36.3	4.5	12.3	5.477	151.6±4.5
5	69.7	0.2	11.5	3.523	99.0±86.8
	22.9	4.0	14.9	5.878	162.2±3.4
6	32.6	0.3	5.8	4.319	120.6±51.1
	38.0	3.5	8.5	5.521	152.8±4.9
7	88.4	0.3	8.7	4.691	130.6±41.2
	53.9	5.1	9.3	5.454	151.0±3.3
8	80.8	0.4	6.3	5.622	155.5±34.0
	46.2	5.3	8.0	5.336	147.9±4.4
9	47.2	0.3	8.8	5.321	147.5±50.4
	49.8	0.5	14.1	3.875	108.6±32.1
10	76.2	0.2	9.6	3.448	96.9±71.2
	39.5	3.4	13.4	5.430	150.4±3.4
11	85.6	0.3	9.2	2.887	81.5±44.8
	50.9	2.6	11.8	5.007	139.1±5.5
VO181 Plagioclase, small bulk sample, 1.00 mg (J=0.01658)					
1	86.8	0.5	4.2	4.428	128.0±26.1
2	80.7	0.9	6.3	2.463	72.3±13.0
3	64.0	2.0	9.0	3.293	96.0±7.6
4	28.2	4.2	13.3	4.794	138.2±3.4
5	15.7	5.7	14.8	5.236	150.4±1.8
6	9.7	6.9	15.1	5.298	152.1±1.8
7	7.1	6.7	15.2	5.470	156.8±1.7
8	7.3	6.2	15.3	5.547	158.9±1.8
9	9.8	6.3	14.8	5.460	156.6±1.7
10	9.1	5.9	15.1	5.581	159.9±2.0

Table 1 (continued)

Step number or T (°C)	Atmospheric (%)	^{39}Ar (%)	$^{37}Ar_{Ca}/^{39}Ar_K$	$^{40}Ar^*/^{39}Ar_K$	Age±1σ (Ma)
11	9.5	6.4	15.0	5.570	159.6±1.9
12	10.3	5.7	15.0	5.592	160.2±2.2
13	14.3	4.7	15.0	5.427	155.6±2.5
14	8.4	9.4	15.1	5.599	160.4±1.5
15	6.9	8.1	15.2	5.683	162.7±1.7
16	7.9	8.1	5.6	5.579	159.8±1.9
17	7.4	4.3	5.5	5.542	158.8±3.2
18	8.5	8.2	5.7	5.696	163.0±1.9
DTA-740 Amphibole, bulk sample, 10.00 mg (J=0.01649)					
800	101.2	0.00	0.0	–	–±–
900	3.9	0.05	13.9	13.864	372.0±124.4
950	0.0	0.24	6.8	6.763	191.0±32.1
1,000	26.8	3.76	4.6	4.606	132.3±2.1
1,050	17.3	66.72	4.8	4.804	137.7±0.7
1,080	21.9	6.66	4.8	4.765	136.7±1.2
1,110	15.2	16.19	4.7	4.747	136.2±0.8
1,140	24.2	2.05	4.3	4.341	124.9±4.7
1,180	24.5	1.07	4.7	4.711	135.2±9.2
1,250	19.7	2.88	4.5	4.540	130.4±2.8
1,400	35.8	0.37	5.4	5.376	153.4±20.0
1,550	0.0	0.0	966.5	966.485	5107.2±5146.6
RL536-3 Actinolite, bulk sample, 20.70 mg (J=0.01637)					
550	100.6	0.01	0.0	–	–±–
650	101.9	0.64	0.0	–	–±–
700	101.3	1.26	0.0	–	–±–
750	100.6	0.98	0.0	–	–±–
800	103.2	0.97	0.0	–	–±–
880	96.5	3.62	2.0	1.997	58.0±16.9
900	42.2	10.39	5.6	5.638	159.2±2.6
930	15.3	44.76	5.9	5.889	166.0±1.3
960	22.8	17.02	5.7	5.745	162.1±1.6
990	55.2	5.47	5.5	5.522	156.1±3.5
1,030	53.5	9.12	5.4	5.368	151.9±3.1
1,130	46.2	3.96	5.5	5.453	154.2±4.2
1,250	40.7	1.76	4.9	4.875	138.5±9.1
1,400	98.6	0.05	1.0	0.967	28.3±297.4
1,550	122.1	0.00	0.0	−394.885	–±–
RL605D (1) Sericite in situ in plagioclase, single grain, 0.05 mg (J=0.01668)					
1	74.4	35.74	4.4	4.421	128.4±5.7
2	47.4	13.71	3.4	3.443	100.8±13.5
3	53.8	9.23	2.5	2.517	74.2±23.7
4	13.9	18.43	4.2	4.245	123.5±15.6
5	30.9	11.79	4.5	4.539	131.7±23.5
6	69.6	11.10	4.9	4.860	140.7±24.0
RL605D (2) Sericite in situ in plagioclase, single grain, 0.05 mg (J=0.01668)					
1	89.1	27.66	4.2	4.175	121.5±10.6
2	37.4	15.83	4.3	4.251	123.6±8.2
3	67.0	56.51	4.4	4.406	128.0±3.5

The inverse isochron ($^{40}Ar/^{36}Ar)_i$ ratio and ages are calculated from the best-fit line (York 1969) on all points. The errors are taken as the 95% confidence limit of York's model-1 fit. MSWD=mean square of weighted deviates=SUMS/(n−2), with *SUMS*=minimum weighted sum of residuals and n=number of points fitted. The GPS coordinates of the samples are indicated (projection South America 56=SA56). Apparent ages of each individual step are given at 1σ.

Step Temperature (°C) or step number for the sample analyzed with furnace or laser-heating systems, respectively, *w.m.a.* weighted mean age, $(^{40}Ar/^{36}Ar)_i$ initial ratio from inverse isochrone.

Table 2 Detailed $^{40}Ar/^{39}Ar$ analytical results obtained on plagioclase, amphibole, sericitized plagioclase, adularia, and actinolite from lava flows and intrusives from the Michilla mining district

Sample	Coordinates			Rock	Mineral	Plateau age (Ma, ±2σ)	w.m.a. (Ma, ±2σ)	Steps in plateau or w.m.a.	% Ar released	Isochrone age (Ma, ±2σ)	$^{40}Ar/^{36}Ar$ intercept (±2σ)	MSWD	Steps in isochrone age	Integrated age (Ma, ±2σ)
	Lat S	Long W	m.a.s.l.											
VO17	70°04′00″	22°44′00″	1790	Granodiorite	Plagioclase	147.1±2.2		3-fuse	96.20	155.0±12.4	248.6±72.4	1.2	3-fuse	146.1±2.4
VO20	70°06′44″	22°43′45″	1718	Granodiorite	Plagioclase	145.5±2.8		3-fuse	97.05	147.0±3.2	287.3±17.7	0.5	3-fuse	145.9±3.0
VO26B (1)	70°10′49″	22°44′30″	950	Lava flow	K-Feldspar	139.6±1.5		4-fuse	92.10	139.2±15.7	295.6±28.9	11.3	4-fuse	139.5±1.4
VO26B (2)	70°10′49″	22°44′30″	950	Lava flow	K-Feldspar	137.6±2.2		5-fuse	85.76	150.5±20.3	274.2±33.0	0.9	5-fuse	138.1±2.2
VO30B (1)	70°13′44″	22°41′33″	850	Lava flow	K-Feldspar		143.8±1.1	5-8	64.68	143.0±8.9	297.9±33.2	1.2	5–8	144.8±0.9
VO30B (2)	70°13′44″	22°41′33″	850	Lava flow	K-Feldspar	145.1±0.7		1-fuse	100.00	145.8±7.1	294.1±40.7	0.8	1-fuse	145.1±0.7
VO31	70°13′44″	22°41′31″	870	Lava flow	Plagioclase		153.7±1.8	1–6	49.59	155.5±1.9	280.3±15.1	0.7	1–6	158.3±1.2
					Plagioclase		163.6±1.8	8-fuse	39.29	No fit	No fit	–	8-fuse	
VO31 (1)	70°13′44″	22°41′31″	870	Lava flow	Sericite	157.9±3.8		1-fuse	100.00	158.0±4.4	292.5±40.5	1.2	1-fuse	157.9±3.8
VO31 (2)	70°13′44″	22°41′31″	870	Lava flow	Sericite	154.6±2.6		1–5	90.54	154.9±2.1	284.0±26.1	0.6	1–5	153.5±2.8
VO148	70°14′13″	22°41′35″	739	Lava flow	Plagioclase	159.9±1.0		5-fuse	85.60	166.2±2.5	141.2±64.8	1.5	5-fuse	159.4±1.1
VO148 (1)	70°14′13″	22°41′35″	739	Lava flow	Sericite	160.9±1.4		3-fuse	95.28	157.7±5.4	371.1±145.6	1.7	3-fuse	160.0±1.5
VO148 (2)	70°15′18″	22°41′35″	739	Lava flow	Sericite	161.2±0.9		3-fuse	97.21	160.8±1.7	301.6±38.7	1.0	3-fuse	160.4±1.0
VO181	70°14′13″	22°43′32″	269	Diorite	Plagioclase	159.6±1.1		7-fuse	79.89	155.23±7.7	381.7±212.7	1.4	7-fuse	155.6±0.5
RS18 (1)	70°10′03″	22°40′44″	650	Diorite	Plagioclase	154.4±3.9		1-fuse	100.00	155.4±9.7	290.9±70.9	0.7	1-fuse	154.4±3.9
RS18 (2)	70°10′03″	22°40′44″	650	Diorite	Plagioclase	153.7±3.2		2-fuse	97.38	167.2±9.8	221.9±48.4	0.9	2-fuse	152.7±3.3
RS18	70°10′03″	22°40′44″	650	Diorite	Sericite		147.8±1.7	8 grains		147.0±1.8	300.0±9.5	0.8	8 grains	142.2±1.6
DTA-740	70°10′03″	22°40′44″	740	Dyke	Amphibole	137.4±1.1		5–7	89.57	134.6±9.7	311.9±103.7	2.5	5–7	137.0±1.2
RL536-3	70°10′03″	22°40′44″	265	Lava flow	Actinolite	163.6±1.9		7–10	77.64	158.8±1.3	279.5±10.5	1.1	7–10	147.1±3.8
RL605D (1)	70°10′03″	22°40′44″	11	Lava flow	Sericite	120.5±11.9		1-fuse	100.00	104.6±23.8	315.1±22.9	1.2	1-fuse	120.5±11.9
RL605D (2)	70°10′03″	22°40′44″	11	Lava flow	Sericite	125.5±7.5		1-fuse	100.00	128.8±5.7	293.6±4.3	0.4	1-fuse	125.5±7.5

The error is at the 1σ level and does not include the error in the value of the *J* parameter. Age calculations are based on the decay constants given by Steiger and Jäger 1977. Correction factors for interfering isotopes were $(^{39}Ar/^{37}Ar)_{Ca}=7.30\times10^{-4}\pm4\%$, $(^{36}Ar/^{37}Ar)_{Ca}=2.82\times10^{-4}\pm1\%$ and $(^{40}Ar/^{39}Ar)_{K}=2.97\times10^{-2}\pm2\%$.

Step Temperature (°C) or step number for the sample analyzed with a furnace system or a laser probe, respectively, $^{40}Ar^{*}$ radiogenic ^{40}Ar, *Ca* and *K* produced by Ca and K neutron interference, respectively, *J* irradiation parameter, *m.a.s.l.* meters above sea level

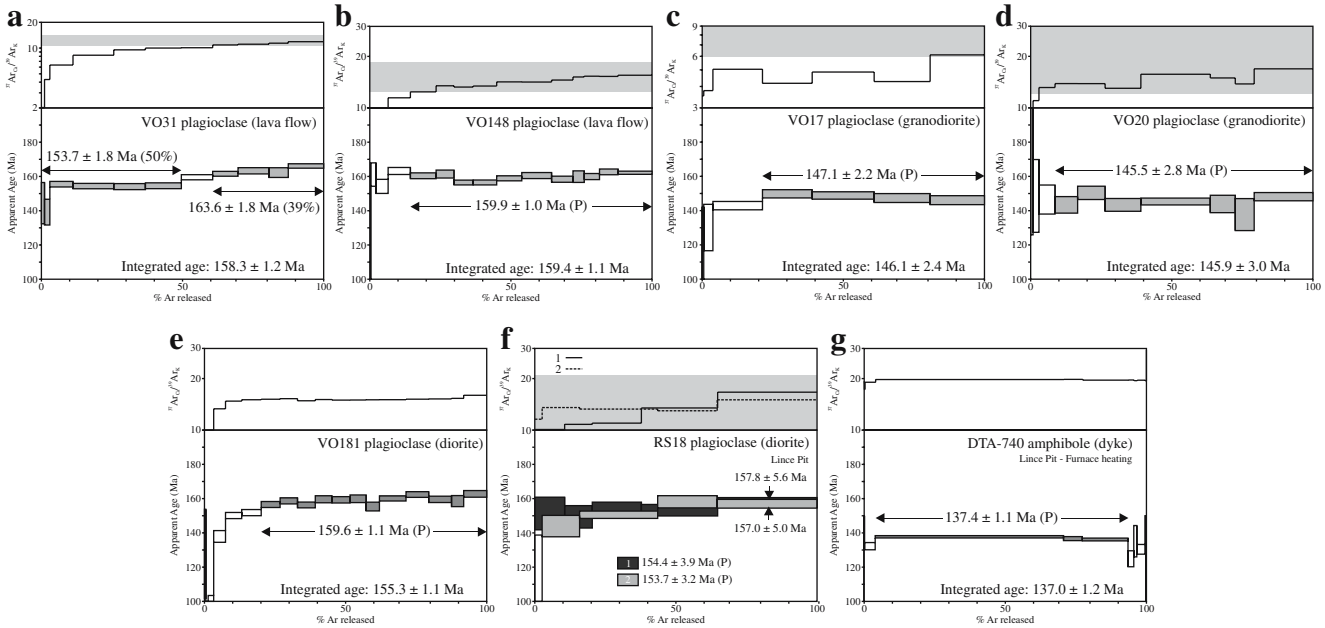

Fig. 4 $^{40}Ar/^{39}Ar$ age and $^{37}Ar_{Ca}/^{39}Ar_K$ ratio spectra obtained on plagioclase and amphibole bulk sample and small plagioclase grain clusters sample from the Michilla district (lava flows: **a**, **b**, **c**; intrusives: **d**, **e**; dyke: **f**). *Shaded rectangles* show $^{37}Ca/^{39}K$ ratios deduced from microprobe analyses (data on Table 3). Plateau and integrated ages are given at the 2-sigma (2σ) confidence level, but apparent ages of each individual step are given at 1σ (Table 1)

Two sericitized plagioclase grains from sample RL605D display concordant plateau ages of 125.5±7.5 and 120.5± 11.9 Ma (Fig. 5e), respectively, but affected by large error bars because of the low sericite content of the grains (high $^{37}Ar_{Ca}/^{39}Ar_K$ ratios).

Actinolite

Actinolite generally occurs as fine needle-shaped crystals infilling amygdales in the lava flows (Fig. 3b). A plateau age of 163.5±1.9 Ma was obtained from a population of amphibole grains from a strongly altered rock (sample RL536-3, Fig. 5f, Table 2). This age may be valid, but it is noteworthy to point out the tiny size of the analyzed minerals (thickness of the needle-shaped crystals <50 μm) and the hump shape of the age spectrum, similar to those generally obtained for glauconite where recoil has been clearly identified (see Hess and Lippolt 1986). Consequently, some ^{39}Ar recoil could have occurred during the irradiation, and therefore the possibility that the obtained age for the actinolite is artificially too old cannot be discarded.

Discussion

Dating volcanic and plutonic events

La Negra Formation lava series

The first magmatic event occurring in the Michilla mining district during Middle Jurassic times was the extrusion of a thick sequence of volcanic rocks, the La Negra Formation, hosting the copper mineralization. Oliveros et al. (2006) demonstrated that plateau ages obtained for fresh plagioclases from altered lava flows of the La Negra Formation probably represent the emplacement age of the lava series because of the coincidence of the obtained ages with the fossil record and the correlation between the alteration degree of the rock and the quality of the age spectra. One plateau age of 159.9±1.0 Ma (VO148) and a high-temperature miniplateau ge of 163.6±1.8 Ma (VO31) corresponding to unaltered plagioclase fractions were obtained for lava flows from the upper third part of the series of the Michilla district. They are concordant with plateau ages of 161.2±1.1, 160.1± 1.5, and 164.9±1.7 Ma obtained from lava flows of the La Negra Formation in the neighboring Tocopilla region, located 40–60 km to the north (Fig. 1) (Oliveros et al. 2006). Unfortunately, a stratigraphic correlation between the two lava series cannot be stablished. The lava flows from the lowest part of the series, hosting the orebodies (Fig. 2), are too altered to be dated.

The intrusions

The plutonic events interpreted from the ages obtained for intrusions and stocks of the Michilla district strictly correspond to the cooling of these intrusive bodies. However, because the size of these bodies is not large, the obtained ages may also represent (considering the large error bars level) the emplacement of the plutonic rocks. This was for example clearly shown for a Cretaceous pluton

in central Chile (Parada et al. 2005). The first plutonic event of a series of three identified pulses of magmatic intrusions in the region is dated at 159.6±1.1 Ma (VO181). This age is close to the plateau ages obtained from plutonic rocks located 30–60 km farther to the north (ca. 155–157 Ma, Oliveros et al. 2006) and which are distributed along a north–south axis along the Coastal Cordillera up to 22°S.

A subvolcanic fine-grained dioritic stock inside Lince pit (sample RS18) was probably emplaced around 158 Ma or slightly before, as suggested by the high temperature apparent ages on slightly altered plagioclase, and could be contemporaneous with the previous pluton (VO181) and upper volcanic lava flows (VO148).

A later plutonic event occurred along the eastern border of the district (Co. Vireira) by plateau ages of 145.5±2.8 and 147.1±2.2 Ma obtained for rocks from a same pluton but sampled in two distinct locations. Similar Earliest Cretaceous ages have been obtained from plutonic rocks

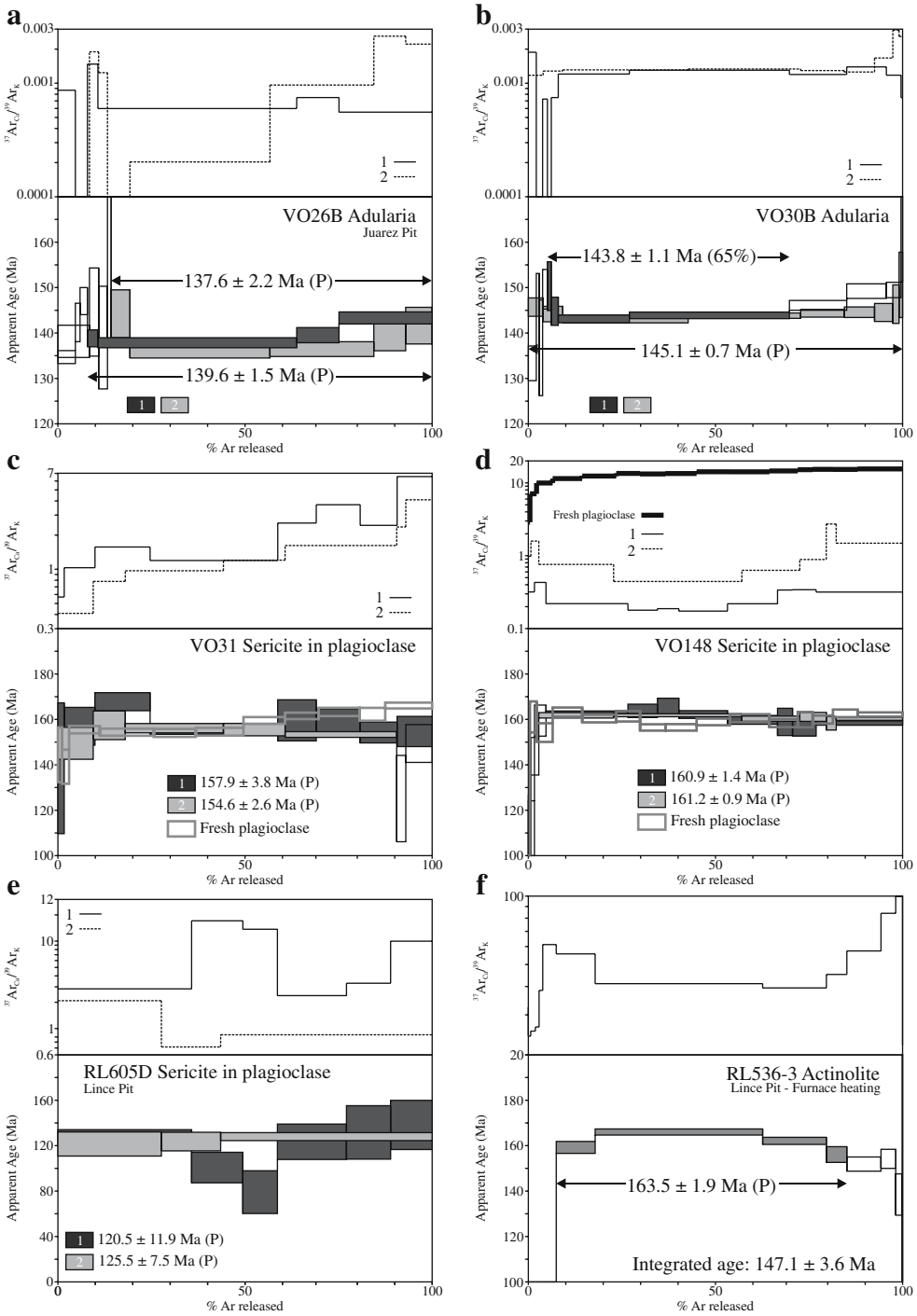

Fig. 5 $^{40}Ar/^{39}Ar$ age and $^{37}Ar_{Ca}/^{39}Ar_K$ ratio spectra obtained for adularia (**a**, **b**) and sericitized plagioclase (**c**, **d**, **e**) single grains and actinolite bulk sample (**f**) from the Michilla district. Plateau and integrated ages are given at the 2-sigma (2σ) confidence level, but apparent ages of each individual step are given at 1σ (Table 1)

Table 3 CaO and K_2O measured from microprobe analyses for fresh plagioclase (inner core)

Sample number	Ca				K				37Ca/39K			
	Min	Max	Mean	±1σ	Min	Max	Mean	±1σ	Min	Max	Mean	±1σ
VO17	4.11	2.51	3.42	0.55	0.24	0.13	0.18	0.03	12.82	6.37	10.31	1.77
VO20	5.63	4.18	4.67	0.45	0.19	0.06	0.13	0.04	49.58	13.21	22.33	10.49
VO31	4.55	0.18	3.09	1.86	4.39	0.18	1.35	1.93	13.59	9.94	12.30	0.89
VO148	4.73	4.33	4.53	0.11	0.18	0.14	0.16	0.01	18.46	13.23	15.89	1.47
RS18	5.49	2.41	4.11	0.66	0.52	0.06	0.18	0.13	53.75	2.51	17.85	11.95

$^{37}Ca/^{39}K$ ratio is calculated as (Ca/K)/1.83.

near Iquique city (21°S) and the Mantos Blancos mining area, at ca. 141–144 Ma (Oliveros et al. 2006, in press).

A still younger intrusive event at 137.4±1.1 Ma (amphibole plateau age) is determined for the andesitic porphyritic dyke from the Lince pit (sample DTA-740) cutting ore bodies. The orientation of these intrusions, mostly perpendicular to the lava flows, indicates that they were emplaced before the extensional tilting of the volcanic sequence. Consequently, this process, which affected the volcanic rocks all along the magmatic arc, would have occurred during the early Cretaceous at least in this region.

Dating alteration events

The ages obtained from alteration minerals are here interpreted as the time interval for the alteration events. Different alteration events have recently been dated by the $^{40}Ar/^{39}Ar$ method in lavas from La Negra Formation in northern Chile (Oliveros 2005). In the Michilla district, the plateau age of 163.6±1.9 Ma obtained from actinolite sample RL536-3 (if valid, as previously discussed) is concordant or close to ages obtained for lava flows from higher stratigraphic levels (see Fig. 2). We observe a concordance between (1)

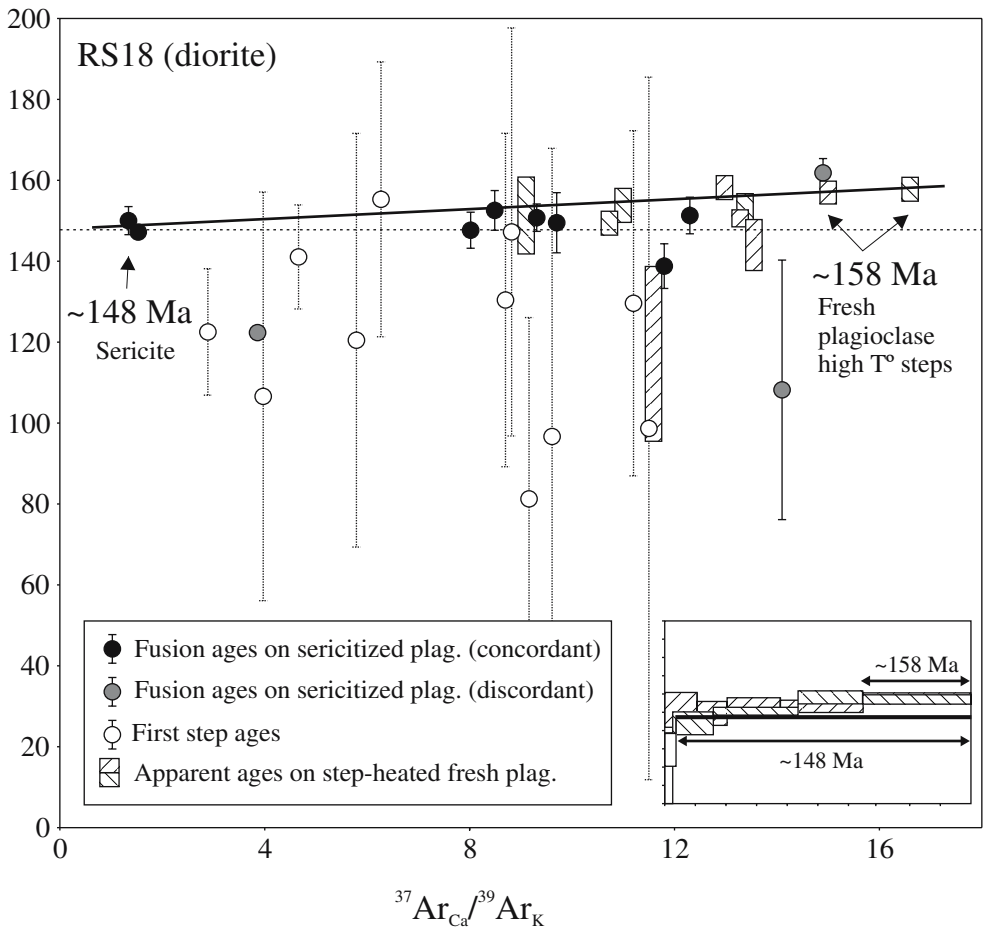

Fig. 6 Apparent age vs $^{37}Ar_{Ca}/^{39}Ar_K$ ratios for two step-heated bulk-sample fresh plagioclase and 11 single grains of sericitized plagioclase from sample RS18. *Filled symbols* represent total fusion steps (~90% of radiogenic Ar released), whereas *empty symbols* represent first low-temperature degassing steps for sericitized single plagioclase grains. *Boxes* represent apparent ages for step-heated fresh plagioclase. *Errors bars* are at the 1σ confidence level (Table 1). *Dotted line* represents the w.m.a. obtained from eight concordant ages. *Heavy line* represents extrapolation between "fresh plagioclase" and "sericite." *Inset*: age spectra for the two bulk sample fresh plagioclase and one grain of sericitized plagioclase

La Negra Formation lava flow emplacement (upper third of the series: 159.9±1.0, 163.6±1.8 Ma), (2) intrusions (plateau age of 159.6±1.1 Ma and high-temperature ages of 157.4±3.6 Ma displayed by VO181 and RS18, respectively), and (3) sericite plateau ages (160.9±1.4 and 161.2±0.9 Ma obtained on VO148). According to these ages, it appears that the secondary event(s) producing sericite in plagioclase is nearly coeval with or immediately follows La Negra Formation volcanism as a consequence of a high fluid/rock ratio in a high thermal gradient environment. These alteration ages appear coincident with the obtained age for actinolite in the deepest levels (Fig. 7).

A slightly younger alteration event seems identified by (1) the "fresh" plagioclase VO31, giving a low temperature miniplateau age of 153.7±1.8 Ma (on gaz fractions from sericitized plagioclase) and (2) plateau ages of 154.6±2.6 and 157.9±3.8 Ma on strongly sericitized single grains (VO31). One (or two) significantly younger alteration events is evidenced by (1) a plateau age of 145.1±0.7 Ma (confirmed by a miniplateau age at 143.8±1.1 Ma) displayed by adularia VO30B from a lava flow from the La Negra series and (2) an age around 148 Ma given by the most sericitized single grains of plagioclase RS18. This event could be related to the emplacement of the huge plutons in the eastern border of the district (Co. Vireira area) giving plateau ages of 147.1±2.2 and 145.5±2.8 Ma on plagioclase.

The alteration event constrained by the plateau ages at 137.6±2.2 and 139.6±1.5 Ma obtained on adularia from a lava flow in the Juarez pit may correspond to other local intrusive events, possibly as that evidenced by dyke DTA-740 (amphibole plateau age of 137.4±1.1 Ma).

A much younger but imprecise alteration event around 126 Ma may be indicated by the barren host rock RL605D. Such an event cannot be connected to any mineralization or intrusive event dated in the district. Nevertheless, if valid, it could correspond to the activation of the sinistral displacement in the Atacama Fault System, which occurred at ca. 125 Ma (Scheuber and González 1999).

The age of Cu mineralization

We examined in detail the relationship between Cu mineralization and the dated alteration minerals. Detailed petrographical and microprobe studies (Tristá-Aguilera 2007) demonstrate that (1) actinolite and chalcocite belong to the same paragenesis (Fig. 3a,b) and precipitated contemporaneously and (2) actinolite crystals have an anomalously high Cu content and thus were likely formed during the Cu mineralization event. Nevertheless, this relationship cannot be extrapolated to the whole deposit because actinolite is a minor alteration phase and coexists with ore minerals only in the deepest levels of the deposit.

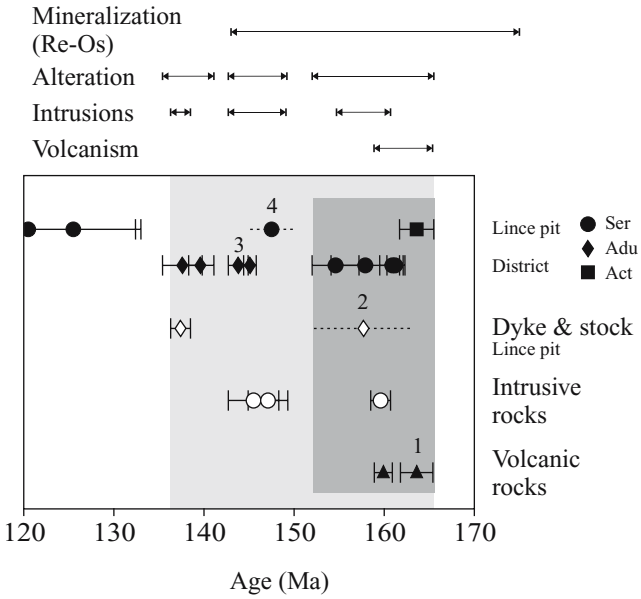

Fig. 7 Synthetic age data of plateau and weighted mean ages obtained on primary and alteration minerals from samples from the Michilla district. *Shaded areas* represent the robustly bracketed (between 157.8±5.6 and 137.4±1.1 Ma, *light gray*) and more precise (between 157.8±5.6 and 163.5±1.9 Ma, *dark gray*) time interval for Cu mineralization. *Ser* Sericite in situ in plagioclase, *Adu* adularia, *Act* actinolite. *1*, High-temperature weighted mean age (VO31); *2*, high-temperature apparent ages (RS18); *3*, weighted mean age (VO30B); and *4*, estimated age for sericite (RS18)

Its formation thus could correspond to an early and punctual stage in the mineralization "history" of the Lince deposit. Therefore, the plateau age of 163.6±1.9 Ma obtained for actinolite sample RL536-3 may represent a mineralization event, although it has been previously outlined that this age should be considered as a maximum age because of the possible recoil effect (see above). This new Ar/Ar age datum and field observations allow the Cu mineralization of the Michilla district to be bracketed between 163.6±1.9 and 137.4±1.1 Ma (Fig. 7), corresponding to the age obtained on actinolite (sample RL536-3) and the postmineralization andesitic barren dyke (sample DTA-740), respectively. This is in agreement with the Re–Os isochrone age of 159±16 Ma (mean square of weighted deviates=1.8) recently obtained by Tristá-Aguilera et al. 2006 on hypogene calcocite–bornite of the Lince–Estefanía pit (Fig. 7), representing the first direct dating of mineralization in Cu-stratabound ore deposits in the Coastal Cordillera of northern Chile.

To tentatively narrow this large age domain, other types of observations may help in giving a possible scenario for the ore minerals formation and age.

1. The small intrusives, as, e.g., the RS18 stock of the Lince–Estefanía pit, are often spatially associated with Cu mineralization; this is also the case for the Buena Esperanza, Buena Vista, and Mantos de la Luna

deposits of the region. It is worth noting that this apparent association is used as a prospection tool.
2. As shown in Fig. 2, the ore bodies (breccia and stratiform) of the Lince–Estefanía pit are located around the intrusive RS18.

These observations suggest that Cu mineralization of the Lince–Estefanía pit belongs to the same magmatic/hydrothermal event(s) as the RS18 intrusion and the actinolite. In this case, the age of the Lince–Estefanía ore deposits would be bracketed between the actinolite plateau age (=maximum age because of eventual recoil) and the high temperature age of 157.4±3.7 Ma measured on the stock RS18 (=minimum age of the stock). Therefore, the Cu mineralization age would be included in the interval ~165–154 Ma (Fig. 7). The validity of this time interval is strengthened by the concordant plateau ages obtained for higher lava flows (located above the RS18 stock) and the actinolite RL536-3 from a lava flow in the mineralization area. This would mean that the Cu mineralization is contemporaneous with or immediately follows the La Negra lava flow emplacement.

The younger ages obtained on secondary minerals not directly associated with Cu mineralization may represent regional scale alteration events, like those described by Losert (1974) and Oliveros (2005) related to the burial of the volcanic pile and/or the intrusion of the Coastal Batholith.

Conclusions

The following are the conclusions obtained from this study:

1. $^{40}Ar/^{39}Ar$ ages obtained for various rock and minerals of the Cu-stratabound Michilla district in the Coastal Cordillera of northern Chile allow the ages of successive magmatic events to be established. The first one corresponds to the thick lavas series of the La Negra Formation, dated at 159.9±1.0 Ma (plateau age on plagioclase VO148) for the upper third of the series, despite the strong alteration affecting the whole series. This data is concordant with plateau ages obtained on the La Negra lava flows from the neighboring Tocopilla region (located 40–60 km to the north; Oliveros et al. 2006).
2. Subcontemporaneous dioritic intrusives were dated at 159.6±1.1 (plateau age on plagioclase VO181) and 157.4 ±3.6 Ma (high-temperature age on plagioclase RS18), close to plateau ages obtained from plutonic rocks located 30–60 km further to the north (ca.155–157 Ma, Oliveros et al. 2006).
3. A second and third intrusive event were dated at 145.5± 2.8 (plagioclase plateau age from a granodioritic pluton: VO20) and 137.4±1.1 Ma (amphibole plateau age on a barren dyke: DTA-740).
4. Secondary minerals gave apparently valid ages because the obtained plateau ages correspond to age data obtained from magmatic rocks of the district (summarized above).
5. An early alteration episode, contemporaneous with the La Negra lava series, is evidenced by actinolite (actinolite+epidote+chlorite+quartz) paragenesis from the deepest levels of the lava series (plateau age of 163.5±1.9 Ma, if valid: sample RL536-3), and strongly sericitized plagioclases from higher lavas (two plateau ages around 161 Ma for sample VO148). According to their stratigraphic positions, a high thermal component is probably the cause of their genesis.
6. A slightly younger alteration event seems to be indicated by strongly sericitized single grains (plateau ages around 155-158 Ma: sample VO31), possibly related to a dated intrusive event (RS18 sample).
7. Later events around 144–145 (plateau ages on the VO30B sample) and 138–140 Ma (plateau ages on the VO26B sample) were evidenced by adularia from the La Negra lava flows, which may be related to two intrusive events in the district mentioned above. A later imprecise alteration event around 126 Ma could be related to the AFS that strongly affects the region.
8. The Cu mineralization of the Michilla district is bracketed between 163.5±1.9 and 137.4±1.1 Ma, corresponding to the ages obtained on actinolite (sample RL536-3) and the postmineralization barren dyke (sample DTA-740), respectively. Furthermore, the observed association of small intrusives, as, e.g., the analyzed RS18 stock, with Cu mineralization of the region, suggests that the main Michilla ore deposit is related to a magmatic/hydrothermal event dated between 163.5± 1.9 and 157.4±3.6 Ma. This event is contemporaneous with or immediately follows the La Negra lava flow emplacement. This age is in agreement with the Re–Os age of 159±16 Ma measured on the mineralization itself (Tristá-Aguilera et al. 2006).

Acknowledgments This work was financially supported by the Institut de Recherche pour le Développement (IDR), a MECESUP-Chile scholarship (D Tristá–Aguilera), and Minera Michilla S.A. Geologists and assistants of the Department of Geology of Minera Michilla S.A are also gratefully thanked for allowing us to undertake this study and its geological contribution. M. Manetti is thanked for analytical assistance. Two anonymous reviewers and J Le Roux are thanked for their helpful comments on the previous version of this manuscript.

References

Acevedo J (2002) Modelamiento unidades geológicas y evolución geológica del yacimiento Lince–Estefanía. Distrito Minero Carolina de Michilla, Segunda Región, Chile. Thesis, Universidad Católica del Norte, Departamento de Ciencias Geológicas, Antofagasta, p 153

Aguirre L, Féraud G, Morata D, Vergara M, Robinson D (1999) Time interval between volcanism and burial metamorphism and rate of basin subsidence in a Cretaceous Andean extensional setting. Tectonophysics 313:433–447

Astudillo O (1983) Geología y metalogénesis del distrito minero Carolina de Michilla, Antofagasta, II Región, Chile. Thesis, Universidad del Norte, Departamento de Geociencias, Antofagasta, p 131

Bogdanic T, Standen R, Wilke H (1994) Nuevos antecedentes de sedimentitas calcáreas intercaladas en la Formación La Negra a la latitud del Distrito Michilla, II Región de Antofagasta. In: Congreso Geológico Chileno 7 Actas, vol. 1, Concepción, pp 414–417

Boric R, Díaz F, Maksaev V (1990) Geología y yacimientos metalíferos de la Región de Antofagasta, bol 40. Servicio Nacional de Geología y Minería, Santiago, p 246

Cembrano J, González G, Arancibia G, Ahumada I, Olivares V, Herrera V (2005) Fault zone development and strain partitioning in an extensional strike–slip duplex: a case study from the Mesozoic Atacama fault system, Northern Chile. Tectonophysics 400:105–125

Chavez W (1985) Geological setting and the nature and distribution of disseminated copper mineralization of the Mantos Blancos district, Antofagasta Province, Chile. Ph.D Thesis, University 611 at California, Berkeley, p 142

Dallmeyer D, Brown M, Grocott J, Taylor G, Treloar PJ (1996) Mesozoic magmatic and tectonic events within the Andean Plate boundary zone, 26°–27°39′S, North Chile: constraints from $^{40}Ar/^{39}Ar$ mineral ages. J Geol 104:19–40

Espinoza S, Orquera W (1988) El yacimiento de cobre Buena Esperanza, geología y alteración de la zona de superficie. Nuevas evidencias sobre edad y génesis, vol 3. Actas 5th Congr Geológico Chileno, Santiago, pp G1–G20

Fuentes F, Féraud G, Aguirre L, Morata D (2005) $^{40}Ar–^{39}Ar$ dating of volcanism and subsequent very low–grade metamorphism in a subsiding basin: example of the Cretaceous lava series from central Chile. Chem Geol 214:157–177

García F (1967) Geología del Norte Grande de Chile, vol 3. Actas Symposium sobre el Geosinclinal Andino, Soc Geológica de Chile, Santiago

Hess JC, Lippolt HJ (1986) Kinetics of Ar isotopes during neutron irradiation: ^{39}Ar loss from minerals as a source of error in $^{40}Ar/^{39}Ar$ dating. Chem Geol Isot Geosci Sect 59:223–236

Jourdan F, Vérati C, Féraud G (2006) Intercalibration of the Hb3gr $^{40}Ar/^{39}Ar$ dating standard. Chem Geol 231:177–189

Kojima S, Astudillo J, Rojo J, Tristá D, Hayashi K (2003) Ore mineralogy, fluid inclusion, and stable isotopic characteristics of stratiform copper deposits in the coastal Cordillera of northern Chile. Miner Dep 38:208–216

Losert J (1974) The formation of stratiform copper deposits in relation to alteration of volcanic series (on north Chilean examples). Rezpravy Československé Akad. Věd. Rocnik 84:1–77

Maksaev V (1990) Metallogeny, geological evolution, and thermochronology of the Chilean Andes between latitudes 21° and 26° south, and the origin of major porphyry copper deposits. Ph.D. thesis, Dalhousie University, Halifax, Nova Scotia, Canada, p 554

Maksaev V (2000) Significado tectónico y metalogénico de datos de trazas de fisión en apatitas de plutones de la Cordillera de la Costa de la Región de Antofagasta, vol 2. Actas 9th Congr Geológico Chileno, Puerto Varas, Chile, pp 129–133

Maksaev V, Zentilli M (2002) Chilean stratabound Cu–(Ag) deposits: an overview. In: Porter TM (ed) Hydrothermal iron oxide copper–gold and related deposits: a global perspective 2. PCG, Adelaide, pp 185–205

Niemeyer H, Standen R, Venegas R (1990) Geología del Distrito Minero Carolina de Michilla. Proyecto de Exploración Geología Distrital. Cía Minera Michilla S.A. Informe Inédito, 195 p

Oliveros V (2005) Etude Géochronologique des Unités Magmatiques Jurassiques et Crétacé Inférieur du Nord du Chili (18°39′–24°S, 60°39′–70°39′W) : Origine, Mise en Place, Altération, Métamorphisme et Minéralisations Associées. Ph.D. thesis, University of Nice, France, University of Chile, Chile p 312.

Oliveros V, Feraud G, Aguirre L, Fornari M (2006) The Early Andean Magmatic Province (EAMP): $^{40}Ar/^{39}Ar$ dating on Mesozoic volcanic and plutonic rocks from the Coastal Cordillera, Northern Chile. J Volcanol Geoth Res 157:311–330

Oliveros V, Ramírez LE, Féraud G, Palacios C, Aguirre L, Parada MA, Fornari M (2007) The Late Jurassic Mantos Blancos major copper deposit, Coastal Range, northern Chile: $^{40}Ar/^{39}Ar$ dating of two overprinted magmatic–hydrothermal breccia-feeding mineralization events. Miner Depos (in press) DOI 10.1007/s00126-007-0146-2

Parada MA, Féraud G, Fuentes F, Aguirre L, Morata D, Larrondo P (2005) Ages and cooling history of the Early Cretaceous Caleu pluton: testimony of a switch from a rifted to a compressional continental margin in central Chile. J Geol Soc Lond 162: 273–287

Pichowiak S (1994) Early Jurassic to Early Cretaceous magmatism in the Coastal Cordillera and the Central Depression of North Chile. In: Reutter KJ, Scheuber E, Wigger PJ (eds) Tectonics of the Southern Central Andes. Structure and evolution of a Continental Margin. Springer-Verlag, Stuttgart, pp 203–217

Renne PR, Swisher CC, Deino AL, Karner DB, Owens T, de Paolo DJ (1998) Intercalibration of standards, absolute ages and uncertainties in $^{40}Ar/^{39}Ar$ dating. Chem Geol 145:117–152

Rogers G (1985) A geochemial traverse across the North Chilean Andes. Ph.D. thesis, Open University, London, p 333

Rogers G, Hawkesworth CJ (1989) A geochemical traverse across the North Chilean Andes: Evidence for crust generation melt from the mantle wedge. Earth Planet Sci Lett 91:271–285

Sato T (1984) Manto type copper deposits in Chile, a review. Bulletin of the Geological Survey of Japan 35:565–582

Scheuber E, González G (1999) Tectonics of the Jurassic–Early Cretaceous magmatic arc of the north Chilean Coastal Cordillera (22°–26°): a story of crustal deformation along a convergent plate boundary. Tectonics 18:895–910

Steiger RH, Jäger E (1977) Subcommission on geochronology: convention on the use of decay constants in geo- and cosmology. Earth Planet Sci Lett 36:359–362

Turner G, Huneke JC, Podose FA, Wasserbrug GJ (1971) $^{40}Ar/^{39}Ar$ ages and cosmic ray exposure ages of Apollo 14 samples. Earth Planet Sci Lett 12:15–19

Tristá-Aguilera D (2007) Procesos geológicos involucrados con la formación de los minerales de mena primarios de los yacimientos estratoligados de Cu: el caso del yacimiento Lince-Estefanía, distrito MIchilla. Segunda región de Antofagasta, Chile. Ph.D. thesis, Northern Catholic University, Antofagasta, p 250

Tristá-Aguilera D, Barra F, Ruiz J, Morata D, Talavera-Mendoza O, Kojima S, Ferraris F (2006) Re–Os isotope systematics for the Lince–Estefanía deposit: constraints on the timing and source of copper mineralization in a stratabound copper deposit, Coastal Cordillera of Northern Chile. Miner Depos 41:99–105

Venegas R, Munizaga F, Tassinari C (1991) Los yacimientos de Cu–Ag del distrito Carolina de Michilla Región de Antofagasta, Chile: nuevos antecedentes geocronológicos, vol 3. Actas 6th Congr Geológico Chileno, Santiago, pp 452–455

Wolf F, Fontboté L, Amstutz G (1990) The Susana copper (–silver) deposit in Northern Chile. Hydrothermal mineralization associated with a Jurassic volcanic arc. In: Fontboté L, Amstutz G, Cardozo M, Cedillo E, Frutos J (eds) Stratabound ore deposits in the Andes. Springer, Berlin, pp 319–338

York D (1969) Least squares fitting of a straight line with correlated errors. Earth Planet Sci Lett 5:320–324